applied sciences

MDPI

Article

An Efficient Code for the Multi-Material Topology Optimization of 2D/3D Continuum Structures Written in Matlab

Ran Zheng [1], Bing Yi [1,*], Xiang Peng [2] and Gil-Ho Yoon [3]

[1] School of Traffic and Transportation Engineering, Central South University, Changsha 410004, China
[2] College of Mechanical Engineering, Zhejiang University of Technology, Hangzhou 310085, China
[3] School of Mechanical Engineering, Hanyang University, Seoul 04763, Republic of Korea
* Correspondence: bingyi@csu.edu.cn

Abstract: This paper presents an efficient and compact Matlab code for 2D and 3D topology optimization of multi-materials. We extend a classical 88-line-based educational code to the multi-material problem using the mapping-based interpolation function, with which each material is modeled equally and can obtain a clear 0, 1 result for each material of the optimized structures that can be manufactured easily. A solution of topology optimization of multi-materials with minimum compliance under volume constraints is documented, including the details of the optimization model, filtering, projection, and sensitivity analysis procedures. Several numerical examples are also conducted to demonstrate the effectiveness of the code, and the influence of the parameter on the optimized results is also analyzed. Complete 2D and 3D Matlab codes are provided.

Keywords: topology optimization; multi-materials; a mapping-based interpolation function; Matlab

check for updates

Citation: Zheng, R.; Yi, B.; Peng, X.; Yoon, G.-H. An Efficient Code for the Multi-Material Topology Optimization of 2D/3D Continuum Structures Written in Matlab. *Appl. Sci.* **2024**, *14*, 657. https://doi.org/10.3390/app14020657

Academic Editor: Lei Wang

Received: 4 December 2023
Revised: 5 January 2024
Accepted: 8 January 2024
Published: 12 January 2024

1. Introduction

Topology optimization of multi-materials is an extension of single-material-based topology optimization and can be used in the structural optimization of components, modules, and also mechanical systems, which has become a hot topic in recent years [1,2]. The challenge of topology optimization of multi-materials is exploring the appropriate mathematical formulation of the interpolation function and the optimization model, which enable each material in the design domain to be completely covered without overlapping, thus being easily manufactured [3–6].

The density-based method is one of the widely used methods for topology optimization of multi-materials, which extends Solid Isotropic Material with Penalization (SIMP), Discrete Material Optimization (DMO), and other interpolation schemes for single materials [7,8]. Sigmund and Torquato [9] first extended the SIMP interpolation method to the multi-material problem and obtained microstructures with extreme thermal expansion. Hvejsel and Lund [10] presented two multi-material interpolation formats that include an arbitrary number of material phases based on the SIMP and Rational Approximation of Material Properties (RAMP) methods [7]. In addition, Stegmann and Lund [11] proposed a discrete material optimization method for the topology optimization of composite structures, which was first adopted for the topology optimization of multi-materials by Gao and Zhang [12]. Bruyneel [13] proposed a shape function parameterization (SFP) method to reduce the number of design variables in DMO. Zhang et al. [7] proposed a multi-material formulation using the ground structure method (GSM) considering material nonlinearity and further derived a ZPR update scheme for topology optimization of truss structures, which is effective for handling multiple constraints of volume/mass. Both the SIMP- and the DMO-based methods used multiple design variables to represent multi-materials, while Yin and Ananthasuresh [14] proposed a peak function that used a linear combination of a normal distribution function for the interpolation function, which only needs one design variable for the topology optimization of multi-materials. Zuo and Saitou [15] proposed an ordered multi-material SIMP interpolation function that only used a single design variable, and the corresponding Matlab code was given. As most of the conventional methods have the problem of gray elements for the optimized structure, especially at the interface between different materials, Yi [16] proposed a mapping-based interpolation function for topology optimization of multi-materials to address these issues, which can obtain precise 0–1 results for each material.

Although many research results have been published for the topology optimization of multi-materials, it is still difficult for new students and researchers to follow the work. An example is the topology optimization of single materials, which was first introduced by Bendsøe and Kikuchi [17] and has been widely used since the 99-line Matlab code was published by Sigmund [18]. There have been many educational papers on single-material topology optimization for different methods such as the SIMP method, the bi-directional evolutionary structural optimization method (BESO), the level set method, the moving morphable components (MMC) method, the homogenization method, and so on. For the SIMP method, Andreassen et al. [19] presented a compact 88-line Matlab code based on the 99-line Matlab code, which improved the calculation speed through matrix operation and also improved filtering strategies. Liu and Tovar [20] presented an efficient and compact 169-line Matlab code to solve three-dimensional topology optimization problems. Later, Sigmund [21] presented new topology optimization Matlab codes for 2D and 3D minimum compliance problems, consisting of 99 and 125 lines, respectively. For the BESO method, Huang and Xie [22] gave a soft-kill BESO Matlab code that can be used to solve simple 2D stiffness optimization problems, which is developed based on the 99-line Matlab code. For the level set method, Vivien and Challis [23] presented a 129-line Matlab code of the level set method for topology optimization, which can be used for multiple load cases. Wei et al. [24] presented an 88-line Matlab code for parameterized level set method-based topology optimization using radial basis functions. For the MMC method, Zhang et al. [25] proposed an ersatz material model and presented a 188-line Matlab code for a topology optimization approach-based MMC framework. Du et al. [26] further extended it to 3D and obtained an easy-to-extend 256-line Matlab code of the MMC method for the topology optimization of 3D structures. For the homogenization method, Xia and Breitkopf [27] presented a Matlab code for the topology optimization of materials with extreme properties based on the 88-line Matlab code. Dong et al. [28] presented a 149-line Matlab code to solve the topology optimization problem with the numerical homogenization method for 3D cellular materials.

There are still more educational papers that we cannot review in this paper, and all of these educational papers have significantly contributed to the development of topology optimization [29]. However, there is little work in educational papers on topology optimization of multi-materials, especially for 3D structures. Tavakoli and Mohseni [30] combined the classical binary phase topology optimization algorithm and the block coordinate descent algorithm and introduced a 115-line Matlab code for solving the multi-material topology optimization problem. Sanders [31] adopted both the ZPR update scheme and the DMO material interpolation scheme for the topology optimization of multi-materials with compliance minimization under volume constraints and presented an educational code named PolyMat by extending the educational code PolyTop. Gangl [32] proposed a level set topology optimization algorithm for multi-materials. The evolution of the design is guided by topological derivatives, which can effectively circumvent the problem of the level set topology optimization method that requires the selection of a perforated initial design. In addition, a Matlab code implementation of an academic multi-material topology optimization problem is also given. However, these focused on 2D problems only, and they are still complex for a new researcher to follow the work.

Hence, we extend the 88-line code for the topology optimization of multi-materials by using the mapping-based interpolation function proposed by Yi [16] in this paper. Implementation with 2D Matlab for the topology optimization of multi-materials with minimum compliance under volume constraints is shown in detail, and compact and complete 2D and 3D Matlab codes are given in the Appendices A and B which will contribute to educating about the topology optimization of multi-materials.

The remainder of this paper is organized as follows. In Section 2, the formulation for topology optimization of multi-materials is described generally, including the filtering, the projection, the mapping-based interpolation function, and the optimization model procedures. A detailed implementation of 2D multi-material topology optimization with Matlab code is presented in Section 3. Then, a number of examples are provided by running the code, as shown in Section 4. An extension of the proposed method to the 3D multi-material topology optimization problem and its numerical examples are presented in Section 5. Finally, conclusions are drawn. Complete Matlab codes are given in the Appendices A and B.

2. The Formulation of the Multi-Material Topology Optimization Problem

2.1. Design Variable

The formulation of the multi-material topology optimization problem based on the mapping-based interpolation function is briefly introduced here for the completeness of this paper. The design domain is usually discretized into finite elements, and each element is assigned a density x_e to determine the material distribution in the topology optimization of continuum structures. Only one design variable is used for the single-material problem, and it is easy to model the interpolation function. The design variable of single materials can be expressed as $x = [x_1, x_2, \cdots x_{n-1}, x_n]^T$, where n is the number of elements used to discretize the design domain. While there are multiple materials that participate in the structural design for multi-material topology optimization problems, the number of design variables for multi-materials is equal to the number of materials multiplied by the number of elements, which can be expressed as:

$$x = \begin{bmatrix} x_1^1 & x_2^1 & \cdots & x_{NM-1}^1 & x_{NM}^1 \\ x_1^2 & x_2^2 & \cdots & x_{NM-1}^2 & x_{NM}^2 \\ \vdots & \vdots & & \vdots & \vdots \\ x_1^{NE-1} & x_2^{NE-1} & \cdots & x_{NM-1}^{NE-1} & x_{NM}^{NE-1} \\ x_1^{NE} & x_2^{NE} & \cdots & x_{NM-1}^{NE} & x_{NM}^{NE} \end{bmatrix} \tag{1}$$

where NE as the superscript of design variables denotes the number of finite elements and NM as the subscript of design variables denotes the multiple materials.

2.2. Filtering and Projection

In order to resolve mesh-dependent and checker-board issues, a density filter is used here [19], which is already provided in the 88-line code.

$$\tilde{x}_i^e = \frac{\sum_{j \in N_e} H_{ej} x_i^j}{\sum_{j \in N_e} H_{ej}} \tag{2}$$

where N_e is the neighborhood of an element x_i^e, which is defined as $N_e = \{j : dist(e, j) \leq R\}$. R is the filter size. H_{ej} is a weight factor, defined as $H_{ej} = max(0, R - dist(e, j))$. $\tilde{x}$ is the filtered density.

To avoid a gray element for the optimized structures and to ensure a 0–1 solution, the *tanh* function-based projection function is used, which can be written as [33,34]:

$$\bar{\tilde{x}}_i^e = \frac{tanh(\beta\eta) + tanh\left(\beta\left(\tilde{x}_i^e - \eta\right)\right)}{tanh(\beta\eta) + tanh(\beta(1-\eta))} \tag{3}$$

where parameter β is used to control the slope of the function; parameter η defines the center of the smooth transition part of the function and is selected as 0.5 in this paper.

2.3. The Mapping-Based Interpolation Function for Multi-Materials

The mapping-based interpolation function is formulated based on the ratio of the p-norm to the 1-norm of the design variables, which was first proposed by Yi [16]. It is simple and clear that the design variable assigned to each element can be directly used as an indicator of whether the corresponding material appears. The Young's moduli of each material interpolated by the mapping-based interpolation function can be expressed as follows:

$$\begin{gathered}
E\left(\overline{\tilde{x}}_1^e, \overline{\tilde{x}}_2^e, \cdots, \overline{\tilde{x}}_{NM}^e\right) = \sum_{i=1}^{NM} (\psi_i)^n (E_i - E_{void}) + E_{void} \\
\psi_i = \frac{\|\overline{\tilde{x}}^e\|_{p-norm}}{\|\overline{\tilde{x}}^e\|_{1-norm} + \delta} \overline{\tilde{x}}_i^e \\
\|\overline{\tilde{x}}^e\|_{p-norm} = ((\overline{\tilde{x}}_1^e)^p + (\overline{\tilde{x}}_2^e)^p + \cdots + (\overline{\tilde{x}}_{NM}^e)^p)^{1/p} \\
\|\overline{\tilde{x}}^e\|_{1-norm} = \overline{\tilde{x}}_1^e + \overline{\tilde{x}}_2^e + \cdots + \overline{\tilde{x}}_{NM}^e
\end{gathered} \tag{4}$$

where ψ_i is the interpolation function and δ is a very small value used to avoid the undefined mathematical operation zero divided by zero. The larger the value of δ, the more it affects the accuracy of the approximation. In application, it is set to be a small value $\delta = 1 \times 10^{-9}$ to balance the accuracy and robustness. In addition, n is a penalization factor, which is used to drive the design variable convergence to 0 or 1. E_i is Young's modulus of the ith material and E_{void} is a very small value representing Young's moduli of void regions. $\left\|\overline{\tilde{x}}^e\right\|_{p-norm}$ and $\left\|\overline{\tilde{x}}^e\right\|_{1-norm}$ are the p-norm and the 1-norm of the projected design variables $\overline{\tilde{x}}_1^e(i = 1, \cdots NM)$, respectively. The influence of the p-norm parameter p will be studied in Section 5.2.

The volume or mass of the structure is often constrained in topology optimization. Therefore, according to the mapping-based interpolation function, the volume or mass constraint for each material can be obtained by the following formula:

$$Mass_i = \sum_{e=1}^{NE} \overline{\tilde{x}}_i^e (i = 1, \cdots NM) \tag{5}$$

2.4. Optimization Model

As usual, the topology optimization of multi-materials with compliance minimization under volume or mass constraints for each material is considered in this paper, which can be written in the following form:

$$\begin{gathered}
min \quad c = F^T U \\
\text{s.t.} \quad V(\overline{\tilde{x}})_i \le V_i^0, i = 1, \cdots NM \\
K(\overline{\tilde{x}})U = F \\
x = \begin{bmatrix}
x_1^1 & x_2^1 & \cdots & x_{NM-1}^1 & x_{NM}^1 \\
x_1^2 & x_2^2 & \cdots & x_{NM-1}^2 & x_{NM}^2 \\
\vdots & \vdots & & \vdots & \vdots \\
x_1^{NE-1} & x_2^{NE-1} & \cdots & x_{NM-1}^{NE-1} & x_{NM}^{NE-1} \\
x_1^{NE} & x_2^{NE} & \cdots & x_{NM-1}^{NE} & x_{NM}^{NE}
\end{bmatrix} \\
0 \le x^{min} \le x \le x^{max} \le 1
\end{gathered} \tag{6}$$

where c is the compliance; K, U, and F represent the stiffness matrix, the displacement, and the force vectors, respectively. $V(\overline{\tilde{x}})_i (i = 1, \cdots NM)$ is the volume of each material, and $V_i^0 (i = 1, \cdots NM)$ is the allowed maximum volume of each material.

The optimization model is iteratively solved by using gradient-based optimization methods such as the method of moving asymptotes (MMA) [35]. The derivations of the sensitivities of the objective function and constraints are outlined in the next section.

2.5. Sensitivity Analysis

The sensitivity of the objective function c with respect to the design variables x can be obtained by the chain rule, which can be computed as follows:

$$\frac{\partial c}{\partial x_i^j} = \frac{\partial c}{\partial \bar{\tilde{x}}_i^e} \frac{\partial \bar{\tilde{x}}_i^e}{\partial \tilde{x}_i^e} \frac{\partial \tilde{x}_i^e}{\partial x_i^j} \tag{7}$$

where the derivative of the objective function c with respect to the projected design variable $\bar{\tilde{x}}$ is:

$$\begin{aligned} \frac{\partial c}{\partial \bar{\tilde{x}}_i^e} &= -U^T \frac{\partial K}{\partial \bar{\tilde{x}}_i^e} U \\ &= -U^T \left(\frac{\partial}{\partial \bar{\tilde{x}}_i^e} \left(\sum_{i=1}^{NM} (\psi_i)^n (E_i - E_{void}) + E_{void} \right) K_0 \right) U \\ &= -U^T \left(\sum_{i=1}^{NM} n(\psi_i)^{n-1} \frac{\partial \psi_i}{\partial \bar{\tilde{x}}_i^e} (E_i - E_{void}) K_0 \right) U \end{aligned} \tag{8}$$

$$\frac{\partial \psi_i}{\partial \bar{\tilde{x}}_i^e} = \frac{((\sum_{j=1}^{NM} (\bar{\tilde{x}}_j^e)^p)^{\frac{1}{p}-1} \cdot (\bar{\tilde{x}}_i^e)^p + (\sum_{j=1}^{NM} (\bar{\tilde{x}}_j^e)^p)^{\frac{1}{p}}) \cdot (\sum_{j=1}^{NM} \bar{\tilde{x}}_j^e + \delta) - ((\sum_{j=1}^{NM} (\bar{\tilde{x}}_j^e)^p)^{\frac{1}{p}} \cdot \bar{\tilde{x}}_i^e}{(\sum_{j=1}^{NM} \bar{\tilde{x}}_j^e + \delta)^2} \tag{9}$$

Moreover, the sensitivity of the volume constraints with respect to the design variables x can also be obtained by the chain rule as:

$$\frac{\partial V(\bar{\tilde{x}})_i}{\partial x_i^j} = \frac{\partial V(\bar{\tilde{x}})_i}{\partial \bar{\tilde{x}}_i^e} \frac{\partial \bar{\tilde{x}}_i^e}{\partial \tilde{x}_i^e} \frac{\partial \tilde{x}_i^e}{\partial x_i^j} \tag{10}$$

$$\frac{\partial V(\bar{\tilde{x}})_i}{\partial \bar{\tilde{x}}_i^e} = 1, \ (i = 1, \cdots NM) \tag{11}$$

In addition, the derivative of the projected density $\bar{\tilde{x}}_i^e$ with respect to the intermediate density $\tilde{x}_i^e$ is given by:

$$\frac{\partial \bar{\tilde{x}}}{\partial \tilde{x}} = \frac{\beta(1 - tanh(\beta(\tilde{x} - \eta)))^2}{tanh(\beta\eta) + tanh(\beta(1 - \eta))} \tag{12}$$

The derivative of the filtered density $\tilde{x}_i^e$ with respect to the design variable x_i^j is calculated as:

$$\frac{\partial \tilde{x}_i^e}{\partial x_i^j} = \frac{H_{ej}}{\sum_{j \in N_e} H_{ej}} \tag{13}$$

3. Matlab Implementation

This section will detail the major modifications from the 88-line Matlab code [19] to 2D multi-material topology optimization problems. Topology optimization of a half MBB beam with three materials is used here to demonstrate the implementation with Matlab code, and the complete 2D Matlab code is provided in Appendix A. The MMA method is implemented with a MATLAB function (mmasub), which can be obtained by contacting Prof. Krister Svanberg from KTH in Stockholm, Sweden (http://www.smoptit.se/ (accessed on 20 January 2023)).

3.1. Parameter Setting (Lines 1–10)

Lines 3–6 define the input parameters required by the program, where `NumIter` is the maximum number of iterations of the algorithm. `delta` is a very small value used to avoid the undefined mathematical operation zero divided by zero. `nelx` and `nely` are the numbers of elements for the finite element method in the horizontal and vertical direction, respectively. `penal` is the penalization factor, which is parameter n in Equation (4). `rmin` is the filter radius, `NMaterial` is the number of materials, `NDV` is the total number of variables for multiple materials of all the elements, and `NDV3` is the number of elements for the finite element method.

Line 7 defines the input parameters required by the MMA algorithm and the projection function. `Movelimit`is used to control the moving limit of the MMA algorithm. `Beta` is the parameter that controls the slope of the projection function. Lines 8–10 define Young's modulus and Poisson's ratio for the three materials.

3.2. Predefined (Lines 1–42)

The preparation of the finite element analysis and the filter is defined in lines 11–42 and is the same as in the 88-line code. The design domain is assumed to be rectangular and is discretized with square elements. The stiffness matrix `lk` of the four-node rectangular element with unit Young's modulus is computed by the code in lines 12–16. The node number, the first-degree number of freedom, and the global degree number of freedom for each element are organized in matrices `nodenrs`, `edofvec`, and `edofMat`, respectively, while matrices `ik` and `jk` contain the rows and columns indices of nonzero entries in the global stiffness matrix. Lines 22–42 are the preparation of the density filter, where the matrix `H` contains the coefficients H_{ej} and `Hs` are normalization constants.

3.3. Initialization (Lines 43–53)

`loopbeta` is a parameter related to the number of iterations, which is initialized to 0 in line 44 so as to adjust the threshold of the projection function according to the iteration number. Design variables x are initially set equal to the prescribed volume fraction in line 45. The projected density $\overline{\tilde{x}}$ corresponding to `xPhys` in line 49 is obtained by filtering and projecting the design variables.

Lines 50–53 initialize some parameters required by the MMA algorithm. The setting of a0, a, cc, and d is based on the mathematical model of this paper. Moreover, `xmin` and `xmax` are the lower and the upper bounds for the variables in line 52, `xold` and `xolder` are the design variable values of the former iterations, while `low` and `upp` are the lower and upper values of the previous iteration in line 53.

3.4. Iterative Solution (Lines 54–137)

These lines are the process of iteratively solving the optimization model, which is the critical part of the implementation. The finite element analysis, the computation of the interpolation function, and the mass constraint for each material are carried out in lines 57–71, whereas the sparse global stiffness matrix is assembled in line 71, as shown in Box 1. The formulation of each material ψ_i is stored in matrix `post_x`, and the constraints are stored in matrix g.

Box 1. Finite element analysis code.

```
57      %% FE-ANALYSIS
58      [KE0] = lk; p=6;
59      for i=1:NMaterial
60         KE(:,:,i)=par.E(i)*KE0;
61      end
62      KE_test=zeros(64,nely*nelx); g=zeros(NMaterial,1);
63      r1=xPhys(:,:,1); r2=xPhys(:,:,2); r3=xPhys(:,:,3);
64      for j=1:NMaterial
65            post_x(1:nely,1:nelx,j)=(xPhys(:,:,j).*(r1.^p + r2.^p +
    r3.^p ).^(1/p))./(r1 + r2 + r3 + delta);
66      dr(1:nely,1:nelx,j)=(post_x(1:nely,1:nelx,j)).^penal;
67      KE_test=reshape(KE(:,:,j),64,1)*reshape(dr(1:nely,1:nelx,j),1,nely*nelx)+KE_test;
68      g(j)=sum((sum(xPhys(:,:,j))'));
69      end
70      sK = reshape(KE_test,64*nelx*nely,1);
71      K = sparse(iK,jK,sK); K = (K+K')/2;
```

The boundary conditions and the load vector of the half MBB beam are defined in lines 72–77. The objective function `c` is computed in lines 79–81, according to the global stiffness matrix `K` and the load vector `F`. The sensitivities `dc` and `dgdx_test` of the objective function and the volume constraints with respect to the projected density are computed in lines 82–100, and then the sensitivities of the filtered and projected procedure are added in lines 101–113, which are stored in `dfdx` and `dgdx`, as shown in Box 2.

Box 2. Sensitivity analysis code.

```
82     %% SENSITIVITY ANALYSIS
83     dc=zeros(nely,nelx,NMaterial);
84     dgdx_test=zeros(NMaterial,nely*nelx*NMaterial);
85     KES=reshape(sum(U(edofMat)*KE0.*U(edofMat),2),nely,nelx);
86     for n=1:NMaterial
87          for m=1:NMaterial
88               if m==n
89                  dmdrn(1:nely,1:nelx,m)=penal.*post_x(1:nely,1:nelx,m).^(penal - 1).*...
90                    ((r1.^p + r2.^p + r3.^p).^(1/p)./(r1 + r2 + r3 + delta) -
                      (xPhys(:,:,m).*(r1.^p + r2.^p + r3.^p).^(1/p))./
                      (r1 + r2 + r3 + delta).^2 + (xPhys(:,:,m).*xPhys(:,:,n).^(p - 1).*
                      (r1.^p + r2.^p + r3.^p).^(1/p - 1))./(r1 + r2 + r3 + delta));
91                  mass_dmdrn=1;
92               else
93                  dmdrn(1:nely,1:nelx,m)=penal.*post_x(1:nely,1:nelx,m).^(penal - 1).*...
94                    (((xPhys(:,:,m).*xPhys(:,:,n).^(p - 1).*(r1.^p + r2.^p + r3.^p).
                      ^(1/p - 1))./(r1 + r2 + r3 + delta)- (xPhys(:,:,m).*(r1.^p +
                      r2.^p + r3.^p).^(1/p))./(r1 + r2 + r3 + delta).^2));
95                  mass_dmdrn=0;
96               end
97                          dgdx_test(m,1+(n-1)*NDV3:NDV3+NDV3*(n-1))=
                            repmat(mass_dmdrn,1,nelx*nely);
98          end
99                         dc(:,:,n)=-dmdrn(:,:,1).*KES.*par.E(1)-dmdrn(:,:,2).
                           *KES.*par.E(2)-dmdrn(:,:,3).*KES.*par.E(3);
100     end
101     %% FILTERING/MODIFICATION OF SENSITIVITIES
102     filtereddc=[];dfdx=[];
103     for i=1:NMaterial
104          dxx = beta * (1-tanh(beta*(xTilde-0.5)).*tanh(beta*(xTilde-0.5)))/
             (tanh(beta*0.5) + tanh(beta*(1-0.5)));
105                    [filtereddc(:,:,i)] = H*(reshape(dc(:,:,i).
                       *dxx(:,:,i),NDV3,1)./Hs);
106          dfdx=[dfdx;filtereddc(:,:,i)];
107          g(i)=(g(i)/NDV3-0.5/3)*1;
108          dgdx1=(dgdx_test(i,:)/NDV3)*1;
109          for j=0:NMaterial-1
110               dgdx2=reshape(dgdx1(:,1+j*NDV3:NDV3+j*NDV3),nely,nelx);
111                    dgdx(i,1+j*NDV3:NDV3+j*NDV3) =
                       H*(reshape(dgdx2(:,:).*dxx(:,:,i),NDV3,1)./Hs);
112         end
113     end
```

The objective function and its sensitivity are scaled to balance the objective and constraints in line 115 if needed, and the movement limits of the MMA algorithm are updated in lines 116–118. The MMA optimization is conducted in lines 119–123, and the intermediate results are displayed in line 125. Parameters are updated in lines 127–136 for the next iteration. The projection function threshold `beta` can be directly changed to a larger value or be gradually increased from a small value. The influence of the two methods will be discussed later. We start with `beta` = 1 and double its value after 50 iterations here.

3.5. Image Display (Lines 138–145)

The final design is displayed in lines 139–144, and the optimized structures with multiple materials are shown in different colors. Finally, the result is saved in line 145, as shown in Box 3.

Box 3. Image Display code.

```
138 %% PLOT DENSITIES
139 xx=post_x(:,:,1);
140 for i=2:NMaterial
141     xx=xx+i*post_x(:,:,i);
142 end
143 imagesc(xx); axis equal; axis off;colorbar; hold on;
144 plot([0 nelx nelx 0 0]+0.5,[0 0 nely nely 0]+0.5, 'k');axis([-1 nelx+1 -1 nely+1])
145 saveas(figure(1), 'result.png');
```

3.6. Visualization of the Optimization Procedure

To demonstrate the usability of the code, Figure 1 shows the final design result as well as the iteration details by calling the code in Appendix A. It can be found that the algorithm can converge stably and quickly to a clear result.

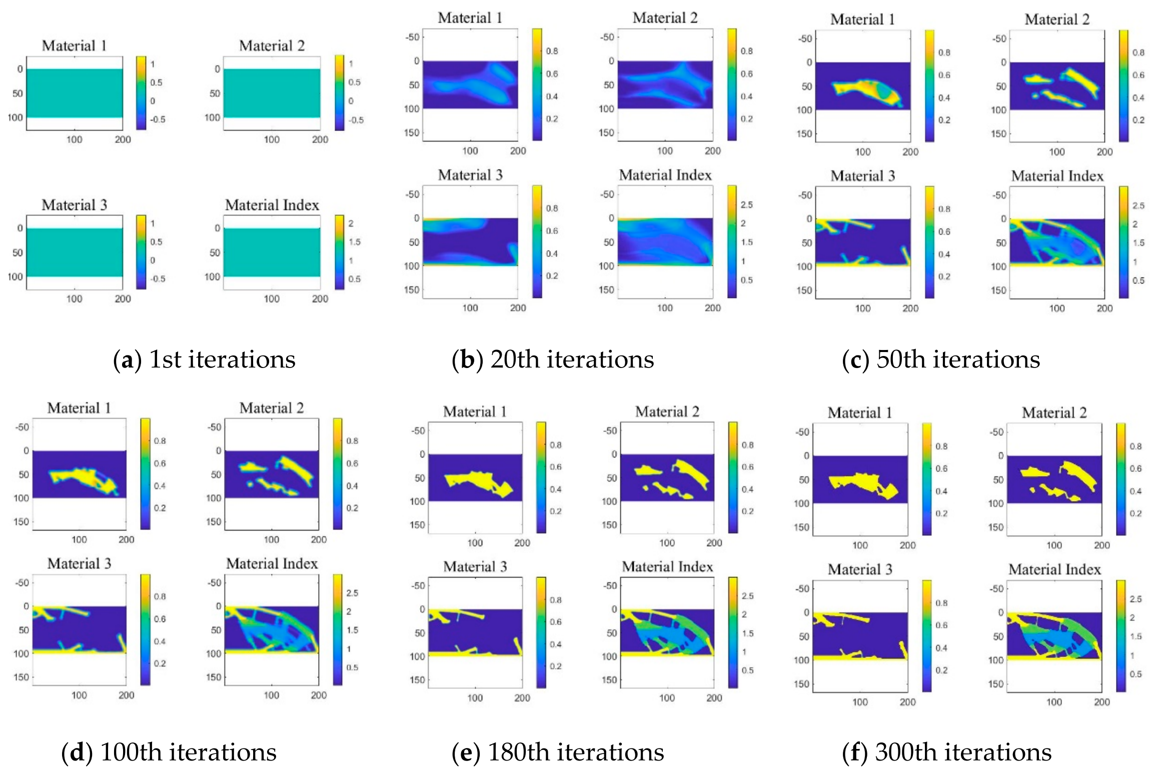

(**a**) 1st iterations (**b**) 20th iterations (**c**) 50th iterations

(**d**) 100th iterations (**e**) 180th iterations (**f**) 300th iterations

Figure 1. The iteration details of the half MBB beam with three materials.

To obtain the results of these intermediate optimization procedures, the code in Box 4 should be inserted after line 132 of the code in Appendix A. The code divides the figure into four sections, with the first three sections showing the density distributions for each of the three materials and the last section showing the results of the current optimized layout of multi-materials.

Box 4. Current image Display code.

```
%% PLOT CURRENT DENSIGN
figure(1);
subplot(2,2,1); imagesc(post_x(:,:,1)); axis equal; colorbar; hold on;
title('Material 1')
subplot(2,2,2); imagesc(post_x(:,:,2)); axis equal; colorbar; hold
on;title('Material 2')
subplot(2,2,3); imagesc(post_x(:,:,3)); axis equal; colorbar;hold
on;title('Material 3')
subplot(2,2,4); xx=post_x(:,:,1);
for i=2:NMaterial
xx=xx+i*post_x(:,:,i);
end
imagesc(2.5); imagesc(xx); axis equal; colorbar; hold on; title('Material Index')
```

4. Numerical Examples

Several numerical examples of the minimum compliance problem are used to illustrate the running results of the Matlab code. The parameters of the above method will affect the final solution similar to conventional methods for topology optimization of continuum structure, and the effect of the parameters is also discussed in this section. The following cases are conducted by using Matlab R2018a on a desktop computer with an Intel CPU 2.8 GHz and 8.0 GB of RAM (Manufacturer: HP, Beijing, China).

4.1. Example 1: The Number of Materials

The half MMB beam is taken as an example for the topology optimization of a continuum structure with two, three, and five materials, respectively. The design domain and boundary conditions of the half MBB beam are shown in Figure 2. A load $F = -1$ is applied at the left upper side of the design domain, and it is simply supported at the bottom corners. The design domain is discretized with 200 × 100 regular elements with Poisson's ratio $\mu = 0.3$. The initial density of each material is set to 0.5.

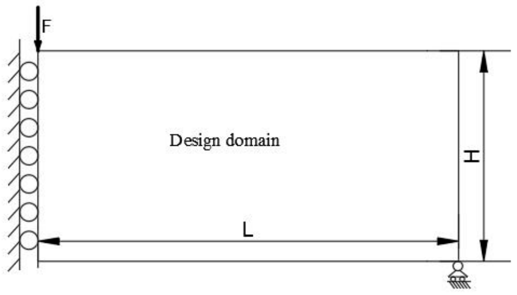

Figure 2. The design domain and boundary conditions of the half MBB beam.

The maximum number of iterations is set as `NumIter = 300`, the penalty factor is set as `penal = 3`, the filter radius is set as `rmin = 5`, and the P-norm parameter p is set as $p = 6$. The parameter for the projection function starts with `beta = 1` and doubles its value after 50 iterations. The volume constraints of two, three, and five materials are set to 0.5/2, 0.5/3, and 0.5/5 for each material, respectively. The Young's modulus of each material for the three cases is set as follows:

Case 1: two materials par.E(1) = 1; par.E(2) = 5;

Case 2: three materials par.E(1) = 1; par.E(2) = 2; par.E(3) = 5;

Case 3: five materials par.E(1) = 1; par.E(2) = 2; par.E(3) = 3; par.E(4) = 4; par.E(5) = 5;

Figure 3 shows the optimized structure and the converged history for topology optimization of different numbers of materials. It can be seen that the code can effectively realize the topology optimization design of multiple materials and obtain clear boundaries for each material. It can be found that the convergence history of the compliance varies little with the number of materials used for optimization, and they converge rapidly in the first 50 iterations. The material volumes also converge rapidly with about 10 iterations. The compliances of the optimized structures for all the cases are almost comparable, and the one with five materials is better than the others, which means that the appropriate layout of multiple materials can improve the stiffness of the optimized structure.

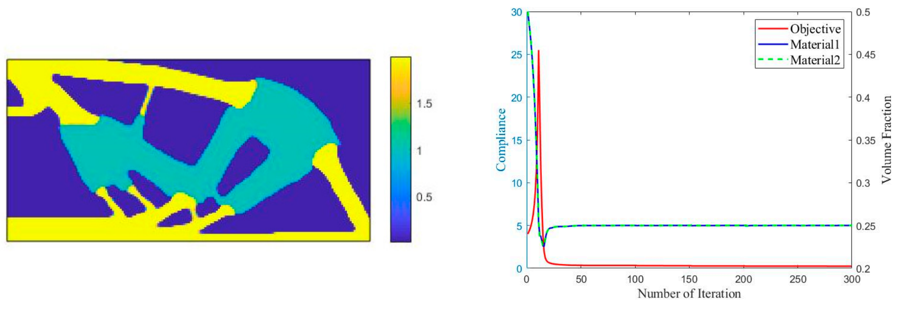

(**a**)

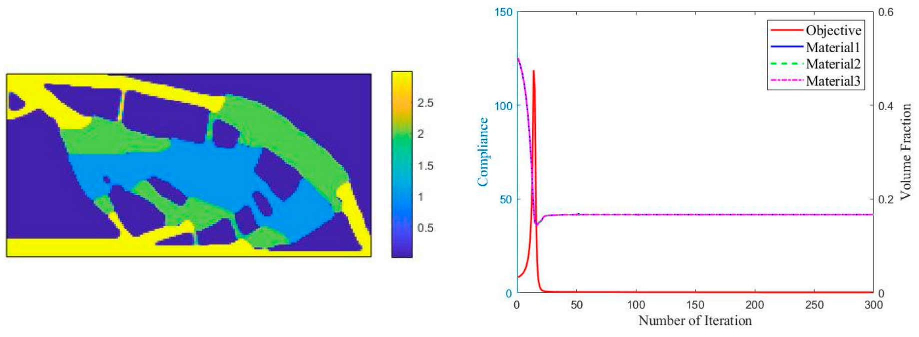

(**b**)

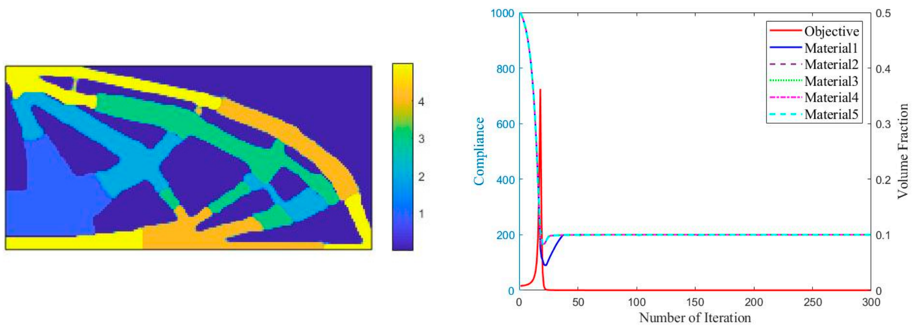

(**c**)

Figure 3. The optimized structure and converge history for topology optimization of different numbers of materials. (**a**) For two materials, the compliance is 0.249, where cyan and yellow are the materials with E = 1 and E = 5, respectively. (**b**) For three materials, the compliance is 0.268, where blue, green, and yellow are the materials with E = 1, E = 2, and E = 5, respectively. (**c**) For five materials, the compliance is 0.242, where blue, cyan, green, orange, and yellow are the materials with E = 1, E = 2, E = 3, E = 4, and E = 5, respectively.

4.2. Example 2: Different Values of Parameter p for the P-Norm

In order to show the influence of the parameter p on the interpolation function of Young's modulus, a diagram of the interpolated Young's modulus $\mathrm{E}\left(\overline{\overline{x}}_1^e, \overline{\overline{x}}_2^e, \cdots, \overline{\overline{x}}_{NM}^e\right)$ as a function of parameter p is shown in Figure 4. Here it is assumed that NM = 2. The Young's modulus of each material is set as $E_1 = 1, E_2 = 5$, with penalty factor n = 3. It can be found that it cannot work well when parameter p is small. As parameter p increases, the interpolated Young's modulus decreases rapidly at the correct part with both design variables equal to 1. Hence, it will drive the optimization model convergence to a clear result of material 1 and material 2 to be voids or solids.

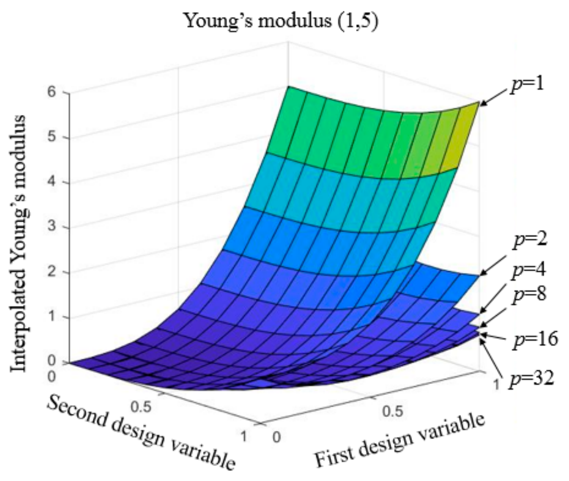

Figure 4. The function diagram of interpolated Young's modulus with respect to parameter p.

To further explore the effect of parameter p on the optimization results, the topology optimization of three materials with the half MMB beam using different P-norm values is also studied. The values of parameter p are set as follows:

Case 1: $p = 1$;

Case 2: $p = 6$;

Case 3: $p = 18$;

Case 4: $p = 32$;

The Young's modulus of each material is set as par.E(1) = 1; par.E(2) = 2; par.E(3) = 5. The volume constraint is set to 0.5/3 for each material, and other parameters are the same as those in Section 4.1. The optimized structures are shown in Figure 5. It can be found that there are mixed materials at the boundary of the optimized structure when $p = 1$ because that p-norm function cannot approximate the maximum of the design variable of Equation (4). By increasing the value of parameter p, the boundary of each material becomes clear for the optimized structure, and the compliance of the optimized structures is comparable. However, it will influence the stability of the optimizer with a very large value of parameter p. Therefore, we choose $p = 6$ in the following examples to balance the structural stiffness and the stability of the optimizer [29].

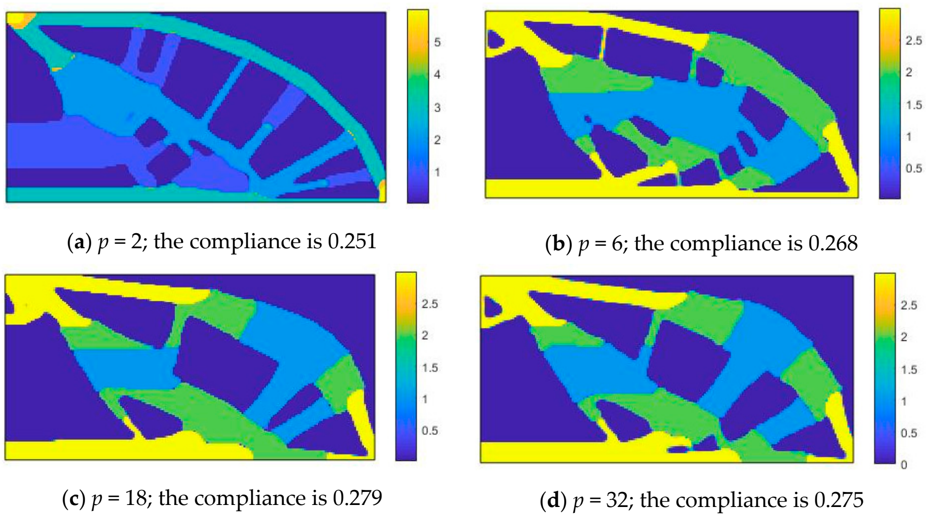
(**a**) $p = 2$; the compliance is 0.251
(**b**) $p = 6$; the compliance is 0.268
(**c**) $p = 18$; the compliance is 0.279
(**d**) $p = 32$; the compliance is 0.275

Figure 5. The optimized structure with different values of parameter p for topology optimization of three materials, where blue, green, and yellow are the materials with E = 1, E = 2, and E = 5, respectively.

5. Extension to 3D

The Matlab implementation described in Section 3 is remarkably easy to extend to 3D problems, which can be found in Appendix B.

5.1. 3D Matlab Implementation

The 3D Matlab implementation is verified using a cantilever beam example here. The boundary conditions and loading conditions for the cantilever beam are shown in Figure 4, and the corresponding Matlab code is defined in lines 11–24. A notable modification compared to the 2D Matlab code is the change in the discrete unit element from four-node rectangle elements to eight-node cubic elements. The element stiffness matrix `lk` is organized in lines 25–40, and the matrix `edofMate` containing the node IDs for each element is obtained in lines 41–44. The iterative details for the three-material cantilever beam can be obtained by calling the code in lines 157–163. The final design is displayed based on the code top3d.m proposed by Liu [20] in lines 164–200, and the optimized structures with multiple materials are shown in different colors.

5.2. 3D Numerical Examples

5.2.1. Example 1: The Number of Materials

The cantilever beam is taken as an example for the topology optimization of a 3D continuum structure with two, three, and five materials, respectively. The design domain and boundary conditions of the 3D cantilever beam are shown in Figure 6. The left part of the design domain is fixed, and a distributed load $F = -1$ is applied at the lower right edge. The design domain is discretized into $80 \times 40 \times 20$ cubic elements with Poisson's ratio $\mu = 0.3$. The initial density of each material is set to 0.5. All other parameters are the same as those in Section 4.1.

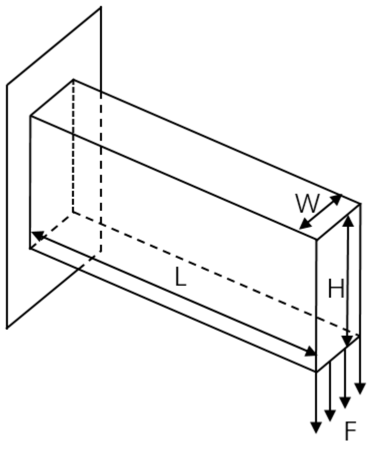

Figure 6. The design domain and boundary conditions of the 3D cantilever beam.

The optimized structure and the converged history for topology optimization of different numbers of materials are shown in Figure 7. It can be found that the convergence histories of the compliance are very similar under different numbers of materials, and they converge rapidly in the first 50 iterations, which is similar to the 2D structures. The compliances of the optimized structure with two materials and the optimized structure with three materials are almost comparable, and the structure with five materials has a smaller compliance value. This is a strong demonstration of the advantages of multiple materials in increasing the stiffness of optimized structures from a three-dimensional perspective.

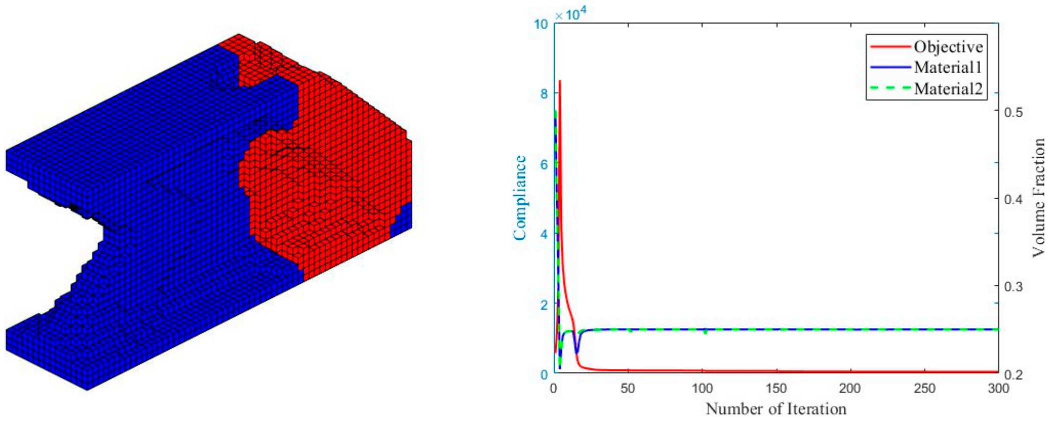

(**a**)

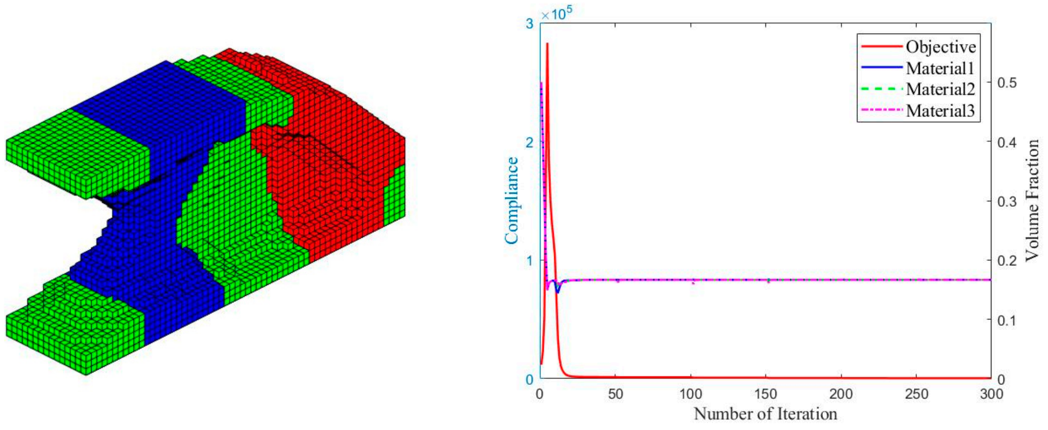

(**b**)

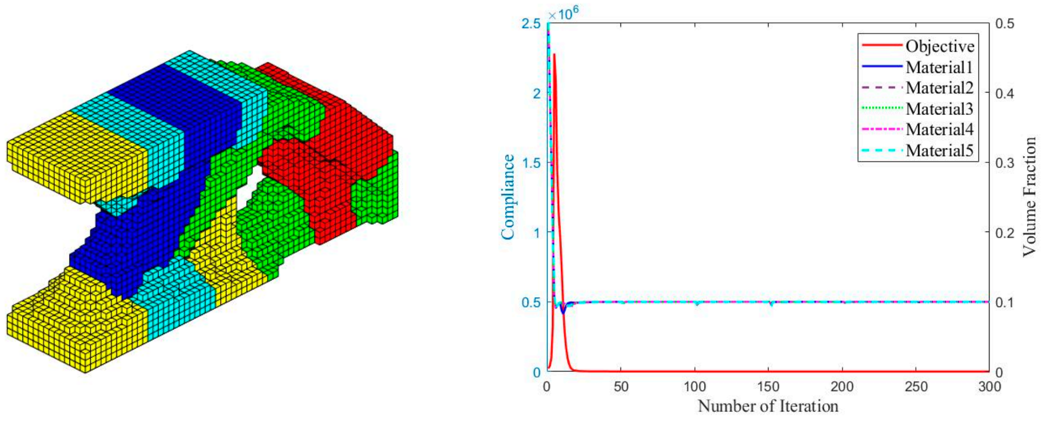

(**c**)

Figure 7. The optimized structure and converge history for topology optimization of multi-materials with 3D cantilever beam. (**a**) For two materials, the compliance is 432.94, where red and blue are materials with E = 1 and E = 5, respectively. (**b**) For three materials, the compliance is 433.05, where red, blue, and green are materials with E = 1, E = 2, and E = 5, respectively. (**c**) For five materials, the compliance is 400.24, where red, blue, cyan, yellow, and green are materials with E = 1, E = 2, E = 3, E = 4, and E = 5, respectively.

5.2.2. Example 2: Different Filter Radii

The topology optimization of the cantilever beam with three materials is taken to test the performance of the code by considering different filter radii to further illustrate the performance of the 3D Matlab code. The filter radii are set as follows:

Case 1: rmin = 2
Case 2: rmin = 5
Case 3: rmin = 8

The Young's moduli are set as par.E(1) = 1; par.E(2) = 2; par.E(3) = 5. The volume constraint is set to 0.5/3 for each material. Other parameters are the same as those in Section 5.2.1. The optimized structures are shown in Figure 8. The results show that the code performs well for feature size control of the optimized structure for topology optimization. Similarly, the topology and the objective function of the optimized structures are changed at different filter radii. As the filter radius is reduced, the advantage of multi-materials is fully utilized with smaller compliance values so that small features can be constructed to get a better local minimum.

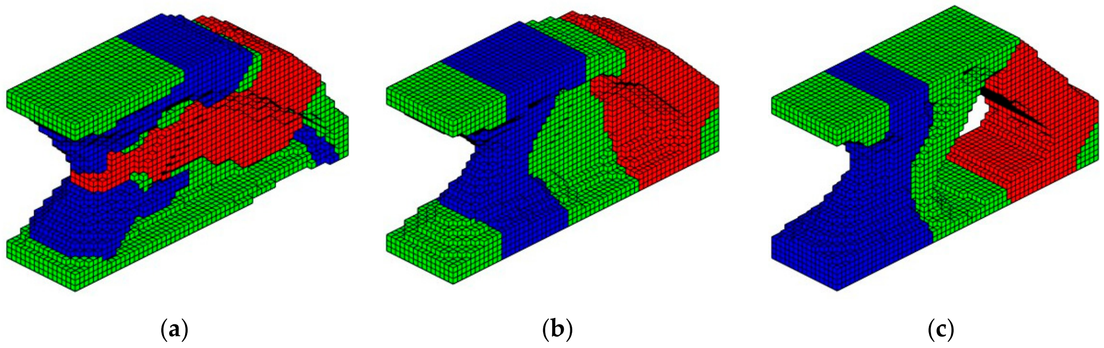

Figure 8. The optimized structure with different filter radii, where red, blue, and green are materials with E = 1, E = 2, and E = 5, respectively. (**a**) For `rmin = 2`, the compliance is 382.46. (**b**) For `rmin = 5`, the compliance is 433.05. (**c**) For `rmin = 8`, the compliance is 539.28.

6. Conclusions

In this paper, simple and efficient 2D and 3D Matlab codes are proposed simultaneously to reduce the barrier of the implementation of multi-material topology optimization. Multi-material topology optimization with the map-based interpolation function proposed by Yi [16] et al. is implemented. The density filter is used to resolve the issues of mesh-dependent and checker-board problems. The projection function is used to ensure a 0–1 solution. The MMA algorithm is used to solve the minimum compliance problem under volume constraints. The algorithm is an extension of the 88-line code for the SIMP-based topology optimization of single materials, and we hope it can provide an educational instrument for newcomers to the field of multi-material topology optimization. Numerical examples of 2D structures with different materials and P-norm parameter p and 3D structures with different materials and filter radii are given to prove the effectiveness of the code.

Author Contributions: Conceptualization, B.Y.; software, R.Z.; validation, X.P. and G.-H.Y.; writing—original draft preparation, R.Z.; writing—review and editing, B.Y.; visualization, X.P. and G.-H.Y. All authors have read and agreed to the published version of the manuscript.

Funding: This work was funded by the Natural Science Foundation of China (No. 51975589) and the Fundamental Research Funds for the Central Universities of Central South University (No. CX20230110).

Institutional Review Board Statement: Not applicable.

Informed Consent Statement: Not applicable.

Data Availability Statement: The data presented in this study are available in the article.

Acknowledgments: The authors thank Daping Li from China Construction Fifth Engineering Division Corp., Ltd. for the discussion of this work.

Conflicts of Interest: The authors declare no conflicts of interest.

Abbreviations

The following abbreviations are used in this manuscript:

SIMP	Solid Isotropic Material with Penalization
DMO	Discrete Material Optimization
RAMP	Rational Approximation of Material Properties
SFP	Shape Function Parameterization
GSM	Ground Structure Method

Appendix A. Multimaterial2d.m

```
%% LOOP PARAMETERS
clear;
NumIter = 300;delta=1e-9;
nelx=200; nely=100;
penal=3; rmin=5; NMaterial=3;
NCON=NMaterial; NDV=nelx*nely*NMaterial; NDV3=nelx*nely;
movelimit=0.1; beta = 1;
%% MATERIAL PROPERTIES
par.E(1)=1; par.E(2)=2; par.E(3)=5;
nu = 0.3;
%% PREPARE FINITE ELEMENT ANALYSIS
A11 = [12 3 -6 -3; 3 12 3 0; -6 3 12 -3; -3 0 -3 12];
A12 = [-6 -3 0 3; -3 -6 -3 -6; 0 -3 -6 3; 3 -6 3 -6];
B11 = [-4 3 -2 9; 3 -4 -9 4; -2 -9 -4 -3; 9 4 -3 -4];
B12 = [ 2 -3 4 -9; -3 2 9 -2; 4 9 2 3; -9 -2 3 2];
lk = 1/(1-nu^2)/24*([A11 A12;A12' A11]+nu*[B11 B12;B12' B11]);
nodenrs = reshape(1:(1+nelx)*(1+nely),1+nely,1+nelx);
edofVec = reshape(2*nodenrs(1:end-1,1:end-1)+1,nelx*nely,1);
edofMat = repmat(edofVec,1,8)+repmat([0 1 2*nely+[2 3 0 1] -2 -1],nelx*nely,1);
iK = reshape(kron(edofMat,ones(8,1))',64*nelx*nely,1);
jK = reshape(kron(edofMat,ones(1,8))',64*nelx*nely,1);
%% PREPARE FILTER
iH = ones(nelx*nely*(2*(ceil(rmin)-1)+1)^2,1);
jH = ones(size(iH));
sH = zeros(size(iH));
k = 0;
for i1 = 1:nelx
    for j1 = 1:nely
         e1 = (i1-1)*nely+j1;
         for i2 = max(i1-(ceil(rmin)-1),1):min(i1+(ceil(rmin)-1),nelx)
              for j2 = max(j1-(ceil(rmin)-1),1):min(j1+(ceil(rmin)-1),nely)
                 e2 = (i2-1)*nely+j2;
                 k = k+1;
                 iH(k) = e1;
                 jH(k) = e2;
                 sH(k) = max(0,rmin-sqrt((i1-i2)^2+(j1-j2)^2));
              end
         end
    end
end
H = sparse(iH,jH,sH);
Hs = sum(H,2);
%% INITIALIZE ITERATION
loopbeta=0;
```

```
x=ones(NDV,1)*0.5;
for i=0:NMaterial-1
   xTilde(1:nely,1:nelx,i+1)=reshape(x(1+i*NDV3:NDV3+i*NDV3),nely,nelx);
end
xPhys = (tanh(beta*0.5) + tanh(beta*(xTilde-0.5)))/(tanh(beta*0.5) + tanh(beta*(1-0.5)));
%% MMA PARAMETER INITIALIZE
a0=0; a=zeros(NCON,1);cc=1.0e6*ones(NCON,1); d=0*ones(NCON,1);
xmin=1e-3*ones(NDV,1); xmax=1*ones(NDV,1);
xold=x; xolder=xold;low=0; upp=1;
%% START ITERATION
for iter=1:NumIter
    loopbeta=loopbeta+1;
    %% FE-ANALYSIS
    [KE0] = lk; p=6;
    for i=1:NMaterial
         KE(:,:,i)=par.E(i)*KE0;
    end
    KE_test=zeros(64,nely*nelx); g=zeros(NMaterial,1);
    r1=xPhys(:,:,1); r2=xPhys(:,:,2); r3=xPhys(:,:,3);
    for j=1:NMaterial
         post_x(1:nely,1:nelx,j)=(xPhys(:,:,j).*(r1.^p + r2.^p + r3.^p ).^(1/p))./(r1 + r2 + r3 + delta);
         dr(1:nely,1:nelx,j)=(post_x(1:nely,1:nelx,j)).^penal;
          KE_test=reshape(KE(:,:,j),64,1)*reshape(dr(1:nely,1:nelx,j),1,nely*nelx)+KE_test;
         g(j)=sum((sum(xPhys(:,:,j))'));
    end
    sK = reshape(KE_test,64*nelx*nely,1);
    K = sparse(iK,jK,sK); K = (K+K')/2;
    %% DEFINE LOADS AND SUPPORTS (HALF MBB-BEAM)
    F = sparse(2*(nely+1)*(nelx+1),1); U = zeros(2*(nely+1)*(nelx+1),1);
    F(2,1) = -0.1;
    fixeddofs = union([1:2:2*(nely+1)],[2*(nelx+1)*(nely+1)]);
    alldofs = [1:2*(nely+1)*(nelx+1)];
    freedofs = setdiff(alldofs,fixeddofs);
    %% SOLVING
    U(freedofs,:)  = K(freedofs,freedofs)\F(freedofs,:);
    U(fixeddofs,:)= 0;
    c=F'*U;
    %% SENSITIVITY ANALYSIS
    dc=zeros(nely,nelx,NMaterial);
    dgdx_test=zeros(NMaterial,nely*nelx*NMaterial);
    KES=reshape(sum(U(edofMat)*KE0.*U(edofMat),2),nely,nelx);
    for n=1:NMaterial
         for m=1:NMaterial
              if m==n
                   dmdrn(1:nely,1:nelx,m)=penal.*post_x(1:nely,1:nelx,m).^(penal -1).*...
                        ((r1.^p + r2.^p + r3.^p).^(1/p)./(r1 + r2 + r3 + delta) -(xPhys(:,:,m).*
                        (r1.^p + r2.^p + r3.^p).^(1/p))./(r1 + r2 + r3 + delta).^2 +
                        (xPhys(:,:,m).*xPhys(:,:,n).^(p -1).*(r1.^p + r2.^p + r3.^p).
                        ^(1/p -1))./(r1 + r2 + r3 + delta));
                   mass_dmdrn=1;
              else
                   dmdrn(1:nely,1:nelx,m)=penal.*post_x(1:nely,1:nelx,m).^(penal -1).*...
                        (((xPhys(:,:,m).*xPhys(:,:,n).^(p -1).*(r1.^p + r2.^p + r3.^p).
                        ^(1/p -1))./(r1 + r2 + r3 + delta)- (xPhys(:,:,m).*(r1.^p + r2.^p + r3.^p).
```

```
                       ^(1/p))./(r1 + r2 + r3 + delta).^2));
                  mass_dmdrn=0;
             end
             dgdx_test(m,1+(n-1)*NDV3:NDV3+NDV3*(n-1))=repmat(mass_dmdrn,1,nelx*nely);
        end
        dc(:,:,n)=-dmdrn(:,:,1).*KES.*par.E(1)-dmdrn(:,:,2).*KES.*par.E(2)-dmdrn(:,:,3).*KES.*par.E(3);
    end
    %% FILTERING/MODIFICATION OF SENSITIVITIES
    filtereddc=[];dfdx=[];
    for i=1:NMaterial
         dxx = beta* (1-tanh(beta*(xTilde-0.5)).*tanh(beta*(xTilde-0.5)))/
         (tanh(beta*0.5) + tanh(beta*(1-0.5)));
         [filtereddc(:,:,i)] = H*(reshape(dc(:,:,i).*dxx(:,:,i),NDV3,1)./Hs);
         dfdx=[dfdx;filtereddc(:,:,i)];
         g(i)=(g(i)/NDV3-0.5/3)*1;
         dgdx1=(dgdx_test(i,:)/NDV3)*1;
         for j=0:NMaterial-1
              dgdx2=reshape(dgdx1(:,1+j*NDV3:NDV3+j*NDV3),nely,nelx);
              dgdx(i,1+j*NDV3:NDV3+j*NDV3) = H*(reshape(dgdx2(:,:).*dxx(:,:,i),NDV3,1)./Hs);
         end
    end
    %% OPTIMALITY CRITERIA UPDATE OF DESIGN VARIABLES AND PHYSICAL DENSITIES
    f=c*1e2; dfdx=dfdx*1e2; cons(iter,1)=g(1);cons(iter,2)=g(2);cons(iter,3)=g(3);
    for j=1:length(x)
         xmin(j)=max(1e-3,x(j)-movelimit); xmax(j)=min(1,x(j)+movelimit);
    end
    %% MMA OPTIZATION
    [xnew, y, z, lamda, ksi, eta, mu, zeta, s, low, upp] = ...
         mmasub(NCON,length(x), iter, ...
         x, xmin, xmax, xold, xolder, ...
         f, (dfdx), g, dgdx, low, upp, a0, a, cc, d);
    %% PRINT RESULTS
    disp(sprintf('Iter.:%3d Obj.:  %8.4e max constraint:  %6.3e', iter, f,max(g)))
    %% UPDATE PARAMETER
    change=norm(abs(xnew-x));
    xolder=xold; xold=x; x = xnew;
    for i=0:NMaterial-1
         xTilde(1:nely,1:nelx,i+1) = reshape((H*xnew(1+i*NDV3:NDV3+i*NDV3,:))./Hs,nely,nelx);
    end
    xPhys = (tanh(beta*0.5) + tanh(beta*(xTilde-0.5)))/(tanh(beta*0.5) + tanh(beta*(1-0.5)));
    if beta < 100 && (loopbeta >= 50)
         beta = 2*beta;loopbeta = 0;
         fprintf('Parameter beta increased to %g.\n',beta);
    end
end
%% PLOT DENSITIES
xx=post_x(:,:,1);
for i=2:NMaterial
    xx=xx+i*post_x(:,:,i);
end
imagesc(xx); axis equal; axis off;colorbar; hold on;
plot([0 nelx nelx 0 0]+0.5,[0 0 nely nely 0]+0.5,'k');axis([-1 nelx+1 -1 nely+1])
saveas(figure(1),'result.png');
```

Appendix B. Multimaterial3d.m

```
%% LOOP PARAMETERS
clear;
NumIter = 300;delta=1e-9;
nelx=60; nely=30; nelz = 15;
penal=3; rmin=5; NMaterial=3;
NDV=nelx*nely*nelz*NMaterial; NDV3=nelx*nely*nelz;
movelimit=0.1; beta =1;
%% MATERIAL PROPERTIES
par.E(1)=1; par.E(2)=2; par.E(3)=5;
nu = 0.3;
%% USER-DEFINED LOAD DOFs
il = nelx; jl = 0; kl = 0:nelz;
loadnid = kl*(nelx+1)*(nely+1)+il*(nely+1)+(nely+1-jl);
loaddof = 3*loadnid(:)  - 1;
%% USER-DEFINED SUPPORT FIXED DOFs
[jf,kf] = meshgrid(1:nely+1,1:nelz+1);
fixednid = (kf-1)*(nely+1)*(nelx+1)+jf;
fixeddofs = [3*fixednid(:); 3*fixednid(:)-1; 3*fixednid(:)-2];
%% DEFINE LOADS AND SUPPORTS (HALF MBB-BEAM)
nele = nelx*nely*nelz;
ndof=3*(nelx+1)*(nely+1)*(nelz+1);
F=sparse(loaddof,1,-1,ndof,1);
U=zeros(ndof,1);
freedofs=setdiff(1:ndof,fixeddofs);
%% PREPARE FINITE ELEMENT ANALYSIS
ke=1/(1+nu)/(2*nu-1)/144 *([-32;-6;-6;8;6;6;10;6;3;-4;-6;-3;-4;-3;-6;10;3;6;8;3;3;4;-3;-3;-32;-6;
 -6;-4;-3;6;10;3;6;8;6;-3;-4;-6;-3;4;-3;3;8;3;...
    3;10;6;-32;-6;-3;-4;-3;-3;4;-3;-6;-4;6;6;8;6;3;10;3;3;8;3;6;10;-32;6;6; -4;6;3;10;-6;-3;10;
    -3;-6;-4;3;6;4;3;3;8;-3;-3;-32;-6;-6;8;6;-6;10;3;3;4;...
    -3;3;-4;-6;-3;10;6;-3;8;3;-32;3;-6;-4;3;-3;4;-6;3;10;-6;6;8;-3;6;10;-3;3;8;-32;-6;6;8;6;-6;8;
    3;-3;4;-3;3;-4;-3;6;10;3;-6;-32;6;-6;-4;3;3;8;-3;...
    3;10;-6;-3;-4;6;-3;4;3;-32;6;3;-4;-3;-3;8;-3;-6;10;-6;-6;8;-6;-3;10;-32;6;-6;4;3;-3;8;-3;3;
    10;-3;6;-4;3;-6;-32;6;-3;10;-6;-3;8;-3;3;4;3;3;-4;6;...
    -32;3;-6;10;3;-3;8;6;-3;10;6;-6;8;-32;-6;6;8;6;-6;10;6;-3;-4;-6;3;-32;6;-6;-4;3;6;10;-3;6;8;
    -6;-32;6;3;-4;3;3;4;3;6;-4;-32;6;-6;-4;6;-3;10;-6;3;...
    -32;6;-6;8;-6;-6;10;-3;-32;-3;6;-4;-3;3;4;-32;-6;-6;8;6;6;-32;-6;-6;-4; -3;-32;-6;-3;-4;-32;
    6;6;-32;-6;-32]+nu*[48;0;0;0;-24;-24;-12;0;-12;0;...
    24;0;0;0;24;-12;-12;0;-12;0;0;-12;12;12;48;0;24;0;0;0;-12;-12;-24;0;-24;0;0;24;12;-12;12;0;
    -12;0;-12;-12;0;48;24;0;0;12;12;-12;0;24;0;-24;-24;0;...
    0;-12;-12;0;0;-12;-12;0;-12;48;0;0;0;-24;0;-12;0;12;-12;12;0;0;0;-24; -12;-12;-12;-12;0;0;48;
    0;24;0;-24;0;-12;-12;-12;-12;12;0;0;24;12;-12;0;...
    0;-12;0;48;0;24;0;-12;12;-12;0;-12;-12;24;-24;0;12;0;-12;0;0;-12;48;0;0;0;-24;24;-12;0;0;-12;
    12;-12;0;0;-24;-12;-12;0;48;0;24;0;0;0;-12;0;-12;...
    -12;0;0;0;-24;12;-12;-12;48;-24;0;0;0;0;-12;12;0;-12;24;24;0;0;12;-12;48;0;0;-12;-12;12;-12;
    0;0;-12;12;0;0;0;24;48;0;12;-12;0;0;-12;0;-12;-12;...
    -12;0;0;-24;48;-12;0;-12;0;0;-12;0;12;-12;-24;24;0;48;0;0;0;-24;24;-12;0;12;0;24;0;48;0;24;0;
    0;0;-12;12;-24;0;24;48;-24;0;0;-12;-12;-12;0;-24;...
    0;48;0;0;0;-24;0;-12;0;-12;48;0;24;0;24;0;-12;12;48;0;-24;0;12;-12;-12;48;0;0;0;-24;-24;48;0;
    24;0;0;48;24;0;0;48;0;0;48;0;48]);
lk(tril(ones(24))==1)=ke';
lk = reshape(lk,24,24 );
lk =lk + lk'- diag( diag( lk ) );
Num_node = (1+nely)*(1+nelx)*(1+nelz);
```

```
nodenrs = reshape(1:Num_node,1+nely,1+nelx,1+nelz);
edofVec = reshape(3*nodenrs(1:end-1,1:end-1,1:end-1)+1,nelx*nely*nelz,1);
edofMat = repmat(edofVec,1,24)+ repmat([0 1 2 3*nely + [3 4 5 0 1 2] -3 -2 -1 3*(nely+1)*(nelx+1)+
[0 1 2 3*nely + [3 4 5 0 1 2] -3 -2 -1]],nele,1);
iK = reshape(kron(edofMat,ones(24,1))',24*24*nele,1);
jK = reshape(kron(edofMat,ones(1,24))',24*24*nele,1);
%% PREPARE FILTER
iH = ones(nele*(2*(ceil(rmin)-1)+1)^2,1);jH = ones(size(iH));sH = zeros(size(iH));
k = 0;
for k1 = 1:nelz
    for i1 = 1:nelx
        for j1 = 1:nely
            e1 = (k1-1)*nelx*nely + (i1-1)*nely+j1;
            for k2 = max(k1-(ceil(rmin)-1),1):min(k1+(ceil(rmin)-1),nelz)
                for i2 = max(i1-(ceil(rmin)-1),1):min(i1+(ceil(rmin)-1),nelx)
                    for j2 = max(j1-(ceil(rmin)-1),1):min(j1+(ceil(rmin)-1),nely)
                        e2 = (k2-1)*nelx*nely + (i2-1)*nely+j2;
                        k = k+1;
                        iH(k) = e1;
                        jH(k) = e2;
                        sH(k) = max(0,rmin-sqrt((i1-i2)^2+(j1-j2)^2+(k1-k2)^2));
                    end
                end
            end
        end
    end
end
H = sparse(iH,jH,sH);
Hs = sum(H,2);
%% INITIALIZE ITERATION
loopbeta=0;
x=ones(NDV,1)*0.5;
for i=0:NMaterial-1
    xTilde(1:nely,1:nelx,1:nelz,i+1)=reshape(x(1+i*NDV3:NDV3+i*NDV3),nely,nelx,nelz);
end
xPhys = (tanh(beta*0.5) + tanh(beta*(xTilde-0.5)))/(tanh(beta*0.5) + tanh(beta*(1-0.5)));
%% MMA PARAMETER INITIALIZE
a0=0; a=zeros(NMaterial,1);cc=1.0e6*ones(NMaterial,1); d=0*ones(NMaterial,1);
xmin=1e-3*ones(NDV,1); xmax=1*ones(NDV,1);
xold=x; xolder=xold;low=0; upp=1;
%% START ITERATION
for iter=1:NumIter
    loopbeta=loopbeta+1;
    %% FE-ANALYSIS
    KE0=lk; p=6;
    for i=1:NMaterial
        KE(:,:,i)=par.E(i)*KE0;
    end
    KE_test=zeros(24*24,nely*nelx*nelz); g=zeros(NMaterial,1);
    r1=xPhys(:,:,:,1); r2=xPhys(:,:,:,2); r3=xPhys(:,:,:,3);
    for j=1:NMaterial
        post_x(1:nely,1:nelx,1:nelz,j)=(xPhys(:,:,:,j).*(r1.^p + r2.^p + r3.^p ).^(1/p))./
        (r1 + r2 + r3+delta);
        dr(1:nely,1:nelx,1:nelz,j)=(post_x(1:nely,1:nelx,1:nelz,j)).^penal;
        KE_test=reshape(KE(:,:,j),24*24,1)*reshape(dr(:,:,:,j),1,nely*nelx*nelz)+KE_test;
        g(j)=sum(sum(sum(xPhys(:,:,:,j))));
    end
    sK = reshape(KE_test,24*24*nelx*nely*nelz,1);
    K = sparse(iK,jK,sK);
    K = (K+K')/2;
     %% SOLVING
     U(freedofs,:)  = K(freedofs,freedofs)\F(freedofs,:);
     U(fixeddofs,:)= 0;
     c=F'*U;
     %% COMPUTE SENSITIVITIES
     dc=zeros(nely,nelx,nelz,NMaterial);
     dgdx_test=zeros(NMaterial,nely*nelx*nelz*NMaterial);
     KES=reshape(sum(U(edofMat)*KE0.*U(edofMat),2),[nely,nelx,nelz]);
     for n=1:NMaterial
          for m=1:NMaterial
               if m==n
                    drmdn(1:nely,1:nelx,1:nelz,m)=penal.*post_x(1:nely,1:nelx,1:nelz,m).^(penal -1).*...
                      ((r1.^p + r2.^p + r3.^p).^(1/p)./(r1 + r2 + r3+delta) -
                      (xPhys(:,:,:,m).*(r1.^p + r2.^p + r3.^p).^(1/p))./(r1 + r2 + r3+delta).^2 +
                      (xPhys(:,:,:,m).*xPhys(:,:,:,n).^(p - 1).*(r1.^p + r2.^p + r3.^p).
                      ^(1/p - 1))./(r1 + r2 + r3+delta));
                    mass_drmdn=1;
               else
             drmdn(1:nely,1:nelx,1:nelz,m)=penal.*post_x(1:nely,1:nelx,1:nelz,m).^(penal - 1).*...
               (((xPhys(:,:,:,m).*xPhys(:,:,:,n).^(p - 1).*(r1.^p + r2.^p + r3.^p).^(1/p - 1))./
               (r1 + r2 + r3+delta)- (xPhys(:,:,:,m).*(r1.^p + r2.^p + r3.^p).^(1/p))./
               (r1 + r2 + r3+delta).^2));
             mass_drmdn=0;
               end
               dgdx_test(m,1+(n-1)*NDV3:NDV3+NDV3*(n-1))=repmat(mass_drmdn,1,nelx*nely*nelz);
          end
          dc(:,:,:,n)=-drmdn(:,:,:,1).*KES.*par.E(1)-drmdn(:,:,:,2).*KES.
          *par.E(2)-drmdn(:,:,:,3).*KES.*par.E(3);
     end
     %% FILTERING/MODIFICATION OF SENSITIVITIES
     filtereddc=[];dfdx=[];
     for i=1:NMaterial
          dxx = beta * (1-tanh(beta*(xTilde-0.5)).*tanh(beta*(xTilde-0.5)))/
          (tanh(beta*0.5) + tanh(beta*(1-0.5)));
          [filtereddc(:,:,:,i)]= H*(reshape(dc(:,:,:,i).*dxx(:,:,:,i),NDV3,1)./Hs);
          dfdx=[dfdx;filtereddc(:,:,:,i)];
          g(i)=(g(i)/NDV3-0.5/NMaterial)*1;
          dgdx1=(dgdx_test(i,:)/NDV3)*1;
          for j=0:NMaterial-1
               dgdx2=reshape(dgdx1(:,1+j*NDV3:NDV3+j*NDV3),nely,nelx,nelz);
               dgdx(i,1+j*NDV3:NDV3+j*NDV3)=H*(reshape(dgdx2(:,:,:).*dxx(:,:,:,i),NDV3,1)./Hs);
          end
     end
     %% OPTIMALITY CRITERIA UPDATE OF DESIGN VARIABLES AND PHYSICAL DENSITIES
     for j=1:length(x)
          xmin(j)=max(1e-3,x(j)-movelimit); xmax(j)=min(1,x(j)+movelimit);
     end
     %% MMA OPTIZATION
     [xnew, y, z, lamda, ksi, eta, mu, zeta, s, low, upp] = ...
          mmasub(NMaterial,length(x), iter, ...
          x, xmin, xmax, xold, xolder, ...
          c, (dfdx), g*1e4, dgdx*1e4, low, upp, a0, a, cc, d);
     %% PRINT RESULTS
     disp(sprintf('Iter.:%3d Obj.:  %8.4e max constraint:  %6.3e', iter,c ,max(g)))
     %% UPDATE PARAMETER
     change=norm(abs(xnew-x));
     xolder=xold; xold=x; x = xnew;
     for i=0:NMaterial-1
          xTilde(1:nely,1:nelx,1:nelz,i+1)= reshape((H*xnew(1+i*NDV3:NDV3+i*NDV3,:))./Hs,nely,nelx,nelz);
     end
     xPhys = (tanh(beta*0.5) + tanh(beta*(xTilde-0.5)))/(tanh(beta*0.5) + tanh(beta*(1-0.5)));
     if beta < 100 && (loopbeta >= 50)
          beta = 2*beta;loopbeta = 0;
     end
     %% PLOT CURRENT MULTI-MATERIAL DENSITIES
     figure(1);
     subplot(2,2,1); display_3D(post_x,1,NMaterial);axis equal; hold on;title('Material 1')
     subplot(2,2,2); display_3D(post_x,2,NMaterial);axis equal; hold on;title('Material 2')
     subplot(2,2,3); display_3D(post_x,3,NMaterial);axis equal; hold on;title('Material 3')
     subplot(2,2,4); display_3D(post_x,4,NMaterial);axis equal; hold on;title('Material Index')
 end
 %% PLOT DENSITIES
 close all;
 display_3D(post_x, NMaterial+1,NMaterial);axis equal; hold on;
 %% 3D TOPOLOGY DISPLAY FUNCTION
 function display_3D(post_x,NMat,Tolnmaterial)
 if NMat<Tolnmaterial+1
     NM=NMat;Nn=NMat;
 else
     NM=NMat-1;Nn=1;
 end
 for Nm=Nn:NM
     [nely,nelx,nelz] = size(post_x(:,:,:,Nm));
     hx = 1; hy = 1; hz = 1;
     face = [1 2 3 4; 2 6 7 3; 4 3 7 8; 1 5 8 4; 1 2 6 5; 5 6 7 8];
     for k = 1:nelz
          z = (k-1)*hz;
          for i = 1:nelx
               x = (i-1)*hx;
               for j = 1:nely
                    y = nely*hy - (j-1)*hy;
                    if (post_x(j,i,k,Nm) >0.5)
                         vert = [x y z; x y-hx z; x+hx y-hx z; x+hx y z; x y z+hx;x y-hx z+hx;
                         x+hx y-hx z+hx;x+hx y z+hx];
                         vert(:,[2 3]) = vert(:,[3 2]); vert(:,2,:)  = -vert(:,2,:);
                         if Nm==1
                           patch('Faces',face,'Vertices',vert,'FaceColor','r');
                         elseif Nm==2
                           patch('Faces',face,'Vertices',vert,'FaceColor','b');
                         elseif Nm==3
                           patch('Faces',face,'Vertices',vert,'FaceColor','g');
                         end
```

```
                    end
               end
          end
     end
end
axis equal; axis tight; axis off; box on; view([-45,30]); hold on;
end
```

References

1. Huang, X.; Li, W. A new multi-material topology optimization algorithm and selection of candidate materials. *Comput. Methods Appl. Mech. Eng.* **2021**, *386*, 114114. [CrossRef]
2. Liu, W.; Yoon, G.H.; Yi, B.; Choi, H.; Yang, Y. Controlling wave propagation in one-dimensional structures through topology optimization. *Comput. Struct.* **2020**, *241*, 106368. [CrossRef]
3. Yang, X.; Li, M. Discrete multi-material topology optimization under total mass constraint. *Comput.-Aided Des.* **2018**, *102*, 182–192. [CrossRef]
4. Bohrer, R.; Kim, I.Y. Multi-material topology optimization considering isotropic and anisotropic materials combination. *Struct. Multidisc. Optim.* **2021**, *64*, 1567–1583. [CrossRef]
5. Liu, B.; Huang, X.; Cui, Y. Topology optimization of multi-material structures with explicitly graded interfaces. *Comput. Methods Appl. Mech. Eng.* **2022**, *398*, 115166. [CrossRef]
6. Chandrasekhar, A.; Suresh, K. Multi-Material Topology Optimization Using Neural Networks. *Comput.-Aided Des.* **2021**, *136*, 103017. [CrossRef]
7. Zhang, X.S.; Paulino, G.H.; Ramos, A.S. Multi-material topology optimization with multiple volume constraints: A general approach applied to ground structures with material nonlinearity. *Struct. Multidisc. Optim.* **2018**, *57*, 161–182. [CrossRef]
8. Shah, V.; Pamwar, M.; Sangha, B.; Kim, I.Y. Multi-material topology optimization considering natural frequency constraint. *Eng. Comput.* **2022**, *39*, 2604–2629. [CrossRef]
9. Sigmund, O.; Torquato, S. Design of materials with extreme thermal expansion using a three-phase topology optimization method. *J. Mech. Phys. Solids* **1997**, *45*, 1037–1067. [CrossRef]
10. Hvejsel, C.F.; Lund, E. Material interpolation schemes for unified topology and multi-material optimization. *Struct. Multidisc. Optim.* **2011**, *43*, 811–825. [CrossRef]
11. Stegmann, J.; Lund, E. Discrete material optimization of general composite shell structures. *Int. J. Numer. Meth. Eng.* **2005**, *62*, 2009–2027. [CrossRef]
12. Gao, T.; Zhang, W. A mass constraint formulation for structural topology optimization with multiphase materials. *Int. J. Numer. Meth. Eng.* **2011**, *88*, 774–796. [CrossRef]
13. Bruyneel, M. SFP—A new parameterization based on shape functions for optimal material selection: Application to conventional composite plies. *Struct. Multidisc. Optim.* **2011**, *43*, 17–27. [CrossRef]
14. Yin, L.; Ananthasuresh, G.K. Topology optimization of compliant mechanisms with multiple materials using a peak function material interpolation scheme. *Struct. Multidiscip. Optim.* **2001**, *23*, 49–62. [CrossRef]
15. Zuo, W.; Saitou, K. Multi-material topology optimization using ordered SIMP interpolation. *Struct. Multidiscip. Optim.* **2017**, *55*, 477–491. [CrossRef]
16. Yi, B.; Yoon, G.H.; Zheng, R.; Liu, L.; Li, D.; Peng, X. A unified material interpolation for topology optimization of multi-materials. *Comput. Struct.* **2023**, *282*, 107041. [CrossRef]
17. Bendsøe, M.P.; Kikuchi, N. Generating optimal topologies in structural design using a homogenization method. *Comput. Methods Appl. Mech. Eng.* **1988**, *71*, 197–224. [CrossRef]
18. Sigmund, O. A 99 line topology optimization code written in Matlab. *Struct. Multidisc. Optim.* **2001**, *21*, 120–127. [CrossRef]
19. Andreassen, E.; Clausen, A.; Schevenels, M.; Lazarov, B.S.; Sigmund, O. Efficient topology optimization in MATLAB using 88 lines of code. *Struct. Multidisc. Optim.* **2011**, *43*, 1–16. [CrossRef]
20. Liu, K.; Tovar, A. An efficient 3D topology optimization code written in Matlab. *Struct. Multidiscip. Optim.* **2014**, *50*, 1175–1196. [CrossRef]
21. Ferrari, F.; Sigmund, O. A new generation 99 line Matlab code for compliance topology optimization and its extension to 3D. *Struct. Multidiscip. Optim.* **2020**, *62*, 2211–2228. [CrossRef]
22. Huang, X.; Xie, Y.-M. A further review of ESO type methods for topology optimization. *Struct. Multidiscip. Optim.* **2010**, *41*, 671–683. [CrossRef]
23. Challis, V.J. A discrete level-set topology optimization code written in Matlab. *Struct. Multidiscip. Optim.* **2010**, *41*, 453–464. [CrossRef]
24. Wei, P.; Li, Z.; Li, X.; Wang, M.Y. An 88-line MATLAB code for the parameterized level set method based topology optimization using radial basis functions. *Struct. Multidiscip. Optim.* **2018**, *58*, 831–849. [CrossRef]
25. Zhang, W.; Yuan, J.; Zhang, J.; Guo, X. A new topology optimization approach based on Moving Morphable Components (MMC) and the ersatz material model. *Struct. Multidiscip. Optim.* **2016**, *53*, 1243–1260. [CrossRef]

26. Du, Z.; Cui, T.; Liu, C.; Zhang, W.; Guo, Y.; Guo, X. An efficient and easy-to-extend Matlab code of the Moving Morphable Component (MMC) method for three-dimensional topology optimization. *Struct. Multidiscip. Optim.* **2022**, *65*, 158. [CrossRef]
27. Xia, L.; Breitkopf, P. Design of materials using topology optimization and energy-based homogenization approach in Matlab. *Struct. Multidiscip. Optim.* **2015**, *52*, 1229–1241. [CrossRef]
28. Dong, G.; Tang, Y.; Zhao, Y.F. A 149 Line Homogenization Code for Three-Dimensional Cellular Materials Written in matlab. *J. Eng. Mater. Technol.* **2019**, *141*, 011005. [CrossRef]
29. Liu, P.; Yan, Y.; Zhang, X.; Luo, Y. A MATLAB code for the material-field series-expansion topology optimization method. *Front. Mech. Eng.* **2021**, *16*, 607–622. [CrossRef]
30. Tavakoli, R.; Mohseni, S.M. Alternating active-phase algorithm for multimaterial topology optimization problems: A 115-line MATLAB implementation. *Struct. Multidiscip. Optim.* **2014**, *49*, 621–642. [CrossRef]
31. Sanders, E.D.; Pereira, A.; Aguiló, M.A.; Paulino, G.H. PolyMat: An efficient Matlab code for multi-material topology optimization. *Struct. Multidiscip. Optim.* **2018**, *58*, 2727–2759. [CrossRef]
32. Gangl, P. A multi-material topology optimization algorithm based on the topological derivative. *Comput. Methods Appl. Mech. Eng.* **2020**, *366*, 113090. [CrossRef]
33. Wang, F.; Lazarov, B.S.; Sigmund, O. On projection methods, convergence and robust formulations in topology optimization. *Struct. Multidiscip. Optim.* **2011**, *43*, 767–784. [CrossRef]
34. Xu, S.; Cai, Y.; Cheng, G. Volume preserving nonlinear density filter based on heaviside functions. *Struct. Multidiscip. Optim.* **2010**, *41*, 495–505. [CrossRef]
35. Svanberg, K. The method of moving asymptotes—A new method for structural optimization. *Numer. Meth. Eng.* **1987**, *24*, 359–373. [CrossRef]